A Proposed Method for Finding Stress and Allowable Pressure in Cylinders with Radial Nozzles

Les M. Bildy

Codeware

ABSTRACT

A simple technique is presented for calculating the local primary stress from internal pressure in nozzle openings. Nozzle internal projections, reinforcing pads and fillet welds are considered for nozzles on cylinders. The technique uses beam on elastic foundation theory and extends the work of W. L. McBride and W. S. Jacobs [7]. A study comparing the proposed method with ASME Section VIII, Division 1 [2] rules and finite element analysis (FEA) is presented for the range of geometries listed in WRC-Bulletin 335. The proposed method predicts a maximum local primary stress that is in good agreement with FEA and burst test data.

INTRODUCTION

Additional provisions dealing with large openings were introduced in ASME VIII-1 beginning with the A95 Addenda of the ASME Code. Difficulties reported in applying Appendix 1-7(b) rules to successful operating vessels prompted the present investigation into the stresses that are present near nozzle-to-cylinder intersections.

The rules listed in ASME VIII-1 paragraph UG-37 give the vessel designer guidance in determining whether the nozzle under consideration is acceptable for internal or external presssure. Experience has shown that the existing Code rules produce designs that are adequate and safe. It should be noted that our collective experience using VIII-1 area replacement rules is based on a design margin of 4.0 on minimum specified tensile strength which prevailed up to January 1, 2000 when a revised margin of 3.5 became effective. As design margins are reduced the need for a more accurate stress analysis at nozzle intersections increases. It is desirable to ensure that plastic deformation does not occur. In addition, detailed local stress information is required in order to satisfy the Code provisions of U-2(g) for nozzles that are subject to external loads.

One solution would be to employ FEA. As a practical matter, proper application of FEA requires that the correct model be used, as outlined by T. P Pastor and J. Hechmer [8], and that the results be properly interpreted. Because of the uncertainties involved in the application of FEA in determining primary stress, WRC-429 tends to discourage the general use of FEA for this purpose. The Code provides no direct method for calculating the magnitude of the primary stress at a nozzle-to-cylinder intersection. The objective of this paper is to propose a simple method to calculate the maximum primary stress produced by internal pressure at nozzle-to-cylinder intersections.

BACKGROUND

Part of the Code rules for area replacement evolved from "*Beams on Elastic Foundation*" Hetenyi [4], which has been used as the accepted method to determine the significance of pressure vessel discontinuities. In particular, the limits of reinforcement specified in the Code are based on a beam on elastic foundation-derived limit for an assumed cylinder geometry of R/T = 10. The classic beam on elastic foundation limit is also based on the assumption that the discontinuity in the cylinder is axisymmetric, i. e., the discontinuity produces a restraint uniform about the circumference. For such a discontinuity the discontinuity stress attenuates with increasing distance and is assumed to be insignificant at a distance of $(RT)^{1/2}/1.285$. The rules in VIII-1 implement the $(RT)^{1/2}/1.285$ consideration in the nozzle wall by specifying that the area contributing be limited to a distance of $2.5t_n$ perpendicular to the vessel. The limit specified in UG-37 for determining the reinforcing area contributed by the cylinder is a function of the nozzle diameter alone. From this it can be inferred that beam on elastic foundation limits are not used in UG-37 for calculating the reinforcement contributed by the cylinder wall. There are also exemptions from UG-37 area replacement requirements for "small" nozzles that depend on nozzle diameter and cylinder thickness with no consideration of vessel diameter.

McBride and Jacobs presented a method to determine the primary stress in large nozzle-to-thin cylinder intersections using beam on elastic foundation limits of reinforcement resisting tension for both the nozzle and cylinder. The McBride and Jacobs method includes consideration of a bending moment that is assumed to be produced by the way the nozzle geometry intersects with the cylinder. The limit assumed to resist this pressure induced nozzle bending is taken to be $[95/(F_y)^{1/2}]T$, rounded to 16T for steel. A modified version of this method is the basis for the VIII-1, Appendix 1-7(b) rules for large openings in cylindrical shells. McBride and Jacobs' work does not specifically address the more common case of smaller nozzles for which the proposed procedure has been developed.

DISCUSSION OF METHOD

The proposed method is based on the assumption of elastic equilibrium. A pressure area calculation similar to the technique used when determining tensile stress when applying VIII-1, Appendix 1-7(b) is employed. It differs from the current Code rules and from McBride and Jacobs in the following ways:

(a) The area in the cylinder near the opening that is considered to reinforce the opening is taken to be a simple function of the shell thickness, namely, 8T for integrally reinforced nozzles, $8(T + t_e)$ for nozzles with "wide" pads, and 10T for all other pad reinforced nozzles. 8T is approximately the tensile half of a noncompact beam having a limiting width-thickness ratio of $[95/(F_y)^{1/2}]T$ (Manual of Steel Construction [5]). It is not a function of the beam on elastic foundation limit $(RT)^{1/2}$ due to the nature of the nozzle discontinuity in the cylinder. This is because a "small" nozzle does not present an axisymmetric discontinuity to the cylinder; hence, $(RT)^{1/2}$ is not an indication of the attenuation distance in the cylinder. However, $(R_n t_n)^{1/2}$ does describe the attenuation distance in the nozzle because the cylinder does restrain the nozzle in an approximately axisymmetric manner.

(b) The maximum local primary membrane stress (P_L) is determined from the calculated average membrane stress using a linear stress distribution. The assumed stress distribution is identical to that produced by a beam subject to a point load at the extreme fiber (see Figure 1). The resulting assumed stress distribution is shown in Figure 2. The stress increases from the hoop stress in the shell, at a distance of L_R from the nozzle, to a maximum value in the shell equal to P_L near the opening. The proposed method is also based on the assumption that the shell discontinuity (opening) produces a uniaxial strain acting in the longitudinal plane of the shell.

(c) The area contributing in the nozzle near the opening is bounded by $[(R_n t_n)^{1/2}]/1.285 + 0.5r_2$ where r_2 is the fillet weld leg size.

(d) Pressure-induced local bending moments are not considered.

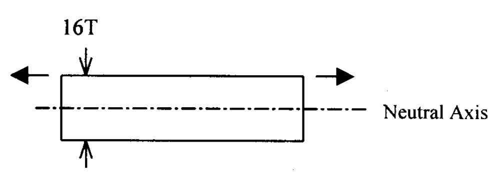

Figure 1
Beam Subject to Point Load

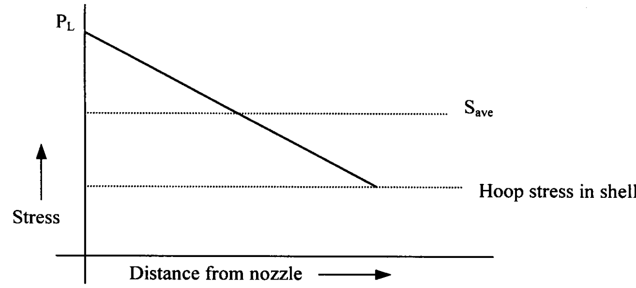

Figure 2
Assumed Stress Distribution at Shell Discontinuity

DESIGN METHOD

Areas contributing to nozzle reinforcement are described in Figure 3:

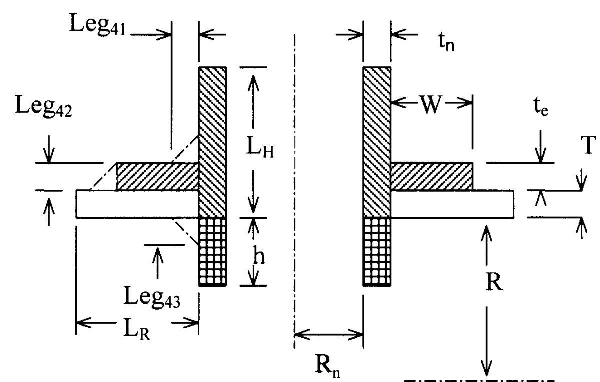

Figure 3
Areas Contributing to Reinforcement

A_1: Area contributed by shell

$$L_R = \text{lesser of } 8T \text{ or } 2(RT)^{1/2} \quad (1)$$

(integrally reinforced or $t_e < 0.5T$)

$$L_R = \text{lesser of } 8(T + t_e) \text{ or } 2(RT)^{1/2} \quad (2)$$

(pad reinforced and $w >= 8(T + t_e)$)

$$L_R = \text{lesser of } 10T \text{ or } 2(RT)^{1/2} \quad (3)$$

(pad reinforced and $w >= 2T$)

$$A_1 = TL_R \quad (4)$$

A_2: Area contributed by nozzle outside vessel

$$L_H = T + t_e + 0.78(R_n t_n)^{1/2} + 0.5Leg_{41} \quad (5)$$

($R_n/R <= 0.7$)

$$L_H = T + t_e + 1.56(R_n t_n)^{1/2} + 0.5Leg_{41} \quad (6)$$

$R_n/R > 0.7$)

$$A_2 = t_n L_H \quad (7)$$

A_3: Area in nozzle inside projection that is contributing

$$A_3 = t_n\{\text{lesser of } h \text{ or } 0.78(R_n t_n)^{1/2} + 0.5\ Leg_{43}\} \quad (8)$$

Area contributed by welds:

$$A_{41} = 0.5Leg_{41}^2 \quad (9)$$

$$A_{42} = 0.5Leg_{42}^2 \quad (10)$$

$$A_{43} = 0.5Leg_{43}^2 \quad (11)$$

A_5: Area contributed by pad

$$A_5 = wt_e, \quad (12)$$

$$w <= L_R$$

f_N: force in nozzle outside of vessel

$$f_N = PR_n(L_H - T) \quad (13)$$

f_S: force in shell

$$f_S = PR(L_R+t_n) \quad (14)$$

f_Y: force due to discontinuity (finished opening in the shell)

$$f_Y = PRR_n \quad (15)$$

S_{ave}: local average primary membrane stress

$$S_{ave} = (f_N + f_S + f_Y) / (A_1 + A_2 + A_3 + A_{41} + A_{42} + A_{43} + A_5) \quad (16)$$

P_L: local maximum primary membrane stress

$$P_L = 2S_{ave} - PR/T \quad (17)$$

Note: Replace T with T + t_e for nozzles with wide pads where w>=8(T+t_e)

Derivation of Nozzle Limit Pressure

A_T: Total tensile area near opening

$$A_T = A_1 + A_2 + A_3 + A_{41} + A_{42} + A_{43} + A_5 \quad (18)$$

F_T: Total tensile force near opening

$$F_T = f_N + f_S + f_Y = P[R_n(L_H - T) + R(L_R + t_n + R_n)] \quad (19)$$

The limiting pressure occurs when $P_L = S_Y = 1.5S$ where S is the allowable stress from Section II, Part D. The limit pressure P for the nozzle can therefore be expressed as

$$P_L = 1.5S = 2S_{ave} - PR/T \quad (20)$$

$$1.5S = 2(F_T/A_T) - PR/T \quad (21)$$

$$1.5S = P[2[R_n(L_H - T) + R(L_R + t_n + R_n)]/A_T - R/T] \quad (22)$$

$$P = 1.5S/[2[R_n (L_H - T) + R(L_R + t_n + R_n)]/A_T - R/T] \quad (23)$$

Note: Replace R/T with R/(T + t_e) in the above expression for nozzles with wide pads where w>= 8(T + t_e).

Summary of Results

Stresses calculated by the proposed method were compared with burst test data from WRC-335 [6] and the results of FEA. Tables 1 and 2 present the results from FEA (P_LFEA) and from the present method (P_LProposed) along with the ratio of the two values. The FEA results were obtained using the FEA-Nozzles computer software program from Paulin Research Group. A plate-shell model, as recommended in Pastor and Hechmer, was used for all FEA calculations. The values for ultimate stress (S_u) and vessel burst pressure (P) were taken from WRC-335. An entry of "burst" in column S_u indicates that the pressure listed in column P was taken from a physical burst test. A numeric entry in column S_u indicates that S_u was used in WRC-335 to calculate the theoretical vessel burst pressure presented here.

ASME VIII-1 area replacement calculations are listed in the A_a/A_r column where A_a is the available area of reinforcement and A_r is the area of reinforcement required. For comparison purposes the allowable stress was taken to be S_u. The ratio A_a/A_r can be taken as an indicator of the accuracy of the VIII-1 calculation. Ideally, the ratio should be 1.0; however, deviation from the ideal ratio is not linear. This is due to the way the VIII-1 shell contributing area A_1 is calculated. VIII-1 A_1 is a function of geometry and pressure. Lowering pressure both decreases area required and increases area available. In WRC-335 and Tables 1 and 2 this has the net effect of making the Code rules appear more conservative. The relationship between nozzle stress and nozzle internal projection was not investigated by either WRC-335 or McBride and Jacobs. Since the proposed method includes consideration of this detail, several FEA comparisons that include a nozzle internal projection were performed.

DISCUSSION OF RESULTS

A review of the results in Table 1 reveals that the proposed method agrees well with both FEA and burst test data from WRC-335 with two notable exceptions. In Table 1 where D_o = 24" the FEA model and WRC-335 indicate a lower stress than the proposed method. A closer examination of the FEA models gives the following possible explanation. In these cases, the region of high stress is not confined to the area near the shell longitudinal axis. One explanation of this is that when the geometry is more flexible, strain redistribution around the circumference of the nozzle occurs. A similar stress distribution was also observed in the FEA models for cases where the R_n/R ratio was larger than about 0.5. The conclusion could be made that the assumption of uniaxial strain breaks down for thin wall vessels having D/T > 200 and for the case of large openings.

It is difficult to find a correlation when comparing the results of the area replacement rules from VIII-1 to FEA in Table 1. One statement that can be made is that the area replacement rules produce results that are more conservative than FEA, burst tests and the proposed method. Beam on elastic foundation theory predicts that nozzles in Table 1 having an R_n/t_n closer to the Code assumed ratio of 10 should be the most accurate for a given R_n/R. The ASME VIII-1 area replacement rules should also become increasingly conservative as R_n/t_n increases beyond 10 for a given R_n/R. There is some evidence of these trends in Table 1.

If the proposed method is valid, then pad reinforced nozzles calculated using ASME VIII-1 rules should result in more accurate results than those observed in Table 1 for integrally reinforced nozzles. This is because both area replacement and the proposed method treat pad reinforcement in similar ways. This is the trend observed in Table 2 where the A_a/A_r ratio is both more consistent and closer to the expected value of 1.0 for WRC-335 burst test and McBride and Jacobs data. In all cases the additional material from internal nozzle projections produced a reduction in stress as expected.

In viewing the FEA models two trends emerged. The region shown by FEA as highly stressed was in all cases confined to a region very near the nozzle. Opening size does not appear to change the stress attenuation distance away from the nozzle. Instead, strain redistribution around the circumference of the nozzle appears. The location of maximum membrane stress for the case of "thick" nozzles or thick reinforcing pads generally seems to occur about 45 degrees from the shell longitudinal axis. Despite this, the magnitude of the stress P_L per the proposed method agrees reasonable well with the FEA results.

The first entry in Table 2 provides an explanation of the unusual failure of the pad reinforced test model noted in WRC-335 3.1.6. E. C. Rodabaugh [6] indicated that the failure location was along the longitudinal axis (WRC-335 location B failure), whereas all other pad reinforced nozzles failed at location A. The proposed method and FEA agree in predicting that failure could occur at location B for this case. Both the proposed method and FEA also agree in predicting that failure would likely not occur at location B for any of the other pad reinforced WRC-335 models investigated.

CONCLUSIONS

The present paper provides several insights into the following VIII-1 design rules for nozzles in cylinders:

Paragraph UG-37

The rules in UG-37 concerning A_1 are based on the nozzle diameter. The present study shows that a more accurate analysis is obtained if the area contributed by the shell is taken to be a function of the shell thickness only. This means that in general the smaller the nozzle the more conservative the Code becomes. This trend indicates that the exemptions found in UG-36(c)(3)(a) are consistent in principle with the findings in this paper. The data in this paper support the conclusion that even with the new higher allowable stresses the Code requires additional reinforcement for many moderately sized nozzles where a more detailed stress analysis would indicate otherwise. In addition to increasing costs, adding more material than required may be detrimental to the fatigue life of the vessel. This effect is more pronounced if the additional reinforcement is provided by a pad.

Paragraph UG-42

Another interesting conclusion concerns the Code provisions for overlapping limits of reinforcement. If the true limit of reinforcement in A_1 is based on the shell thickness alone it follows that the definition of overlapping limits would also be a function of shell thickness. This is an indication that many large nozzles could be closer to other nozzles than is currently assumed.

Appendix 1-7(a)

The large opening rules require that most of the reinforcement be provided near the opening. This is consistent with the findings in this paper. The need for this special provision indicates that the UG-37 assumption concerning limits of reinforcement and nozzle diameter applies to a limited range of geometries. The present study suggests that there are likely two compensating errors at work in these cases. Beam on elastic foundation theory predicts that as R_n/t_n increases beyond 10 the UG-37 rules concerning A_2 become more conservative. At the same time, the area A_1 generally becomes less conservative as R_n increases because the actual limit in the shell is a function of the shell thickness not the nozzle diameter. Whether the outcome is unconservative depends on the thicknesses of the elements involved and the diameter of the opening. Large, relatively thin nozzles on relatively thin shells requiring pad reinforcement are the most likely to experience problems. A "large" nozzle in this context refers to the actual size of the opening, not to the ratio of R_n/R. There have been very few reported problems with large openings designed to Code rules prior to the introduction of Appendix 1-7(b). This is likely because openings large enough to cause this unconservative interaction of the UG-37 rules are rare. An example of such a problem is found in McBride and Jacobs Case 1. Table 2 shows that the 169.24 inch diameter opening meets Appendix 1-7(a) and UG-37 rules for a pressure of 114 psi. Without the provisions of Appendix 1-7(b), local primary membrane stresses in excess of yield (38 ksi for SA-516 70) would be present in the shell.

Appendix 1-7(b)

The proposed method does not consider pressure induced bending moments. In spite of this, the results are in good agreement with the strain gauge measurements reported by McBride and Jacobs. It is the opinion of the author that the pressure induced bending moment is resisted by the attached shell along the outer perimeter of the nozzle. It does not appear that the pressure induced bending moment affects the primary stress analysis of the nozzle at the longitudinal axis.

Nomenclature

A_a	Available area of reinforcement by VIII-1 rules, in^2
A_r	Required area of reinforcement by VIII-rules, in^2
F_y	Material yield stress, ksi
L_H	Stress attenuation distance in nozzle, in
L_R	Stress attenuation distance in shell, in
Leg_{41}	Outer nozzle to shell weld, in
Leg_{42}	Pad to shell weld, in
Leg_{43}	Inner nozzle to shell weld, in
h	Nozzle inside projection, in
P_L	Shell maximum local primary membrane stress, psi
R	Shell inner radius, in
R_n	Nozzle inner radius, in
S_V	Shell allowable stress, psi (VIII-1, UG-37)
S_N	Nozzle allowable stress, psi (VIII-1, UG-37)
S_P	Reinforcing pad allowable stress, psi (VIII-1, UG-37)
S_Y	Yield stress, psi
S	Lesser of shell, nozzle, or pad allowable stress, psi (II-D)
T	Shell thickness, in
t_n	Nozzle thickness, in
t_e	Reinforcing pad thickness, in
w	Reinforcing pad width, in

Acknowledgements

The author would like to express thanks to Professor Gilbert Groendyke of the University of Houston -- Downtown, and Dan McCord of Codeware for their suggestions and assistance with the manuscript.

References

1. ASME Boiler and Pressure Vessel Code, Section II, Part D, 1998 Edition, A99 Addenda

2. ASME Boiler and Pressure Vessel Code, Section VIII, Division 1, 1998 Edition, A99 Addenda.

3. J. L. Hechmer and G. L Hollinger, "3D Stress Criteria Guidelines for Application", Welding Research Council Bulletin 429, Feb. 1998

4. M. Hetenyi, Handbook of Stress Analysis, Wiley, 1957

5. Manual of Steel Construction Allowable Stress Design, Ninth Edition

6. E. C. Rodabaugh, "A review of area replacement rules for pipe connections in pressure vessels and piping," *Weld. Res Counc. Bull. 335*, Aug. 1988. (References to original data sources are given)

7. W. L. McBride and W. S. Jacobs, "Design of Radial Nozzles in Cylindrical Shells for Internal Pressure," *Trans. ASME, J. Pressure Vessel Technol.*, **102**, 70-78, Feb. 1980.

8. T. P. Pastor and J. Hechmer, "ASME Task Group Report on Primary Stress," *Trans. ASME, J. Pressure Vessel Technol.*, **119**, 61-67, Feb. 1997.

Ref No	D_O in	T in	d_O in	t in	P psi	S_u ksi	P_L FEA	P_L proposed	Ratio	A_a/A_r (a)
(5)	12.75	0.375	6.625	0.28	4,100	burst	147.4	148.7	1.009	0.066
(g)	12.75	0.375	6.625	0.28	4,100	65.6	133.7	124.2	0.929	0.251
(5)(c)	12.75	0.375	7.003	0.469	4,100	burst	109.7	117.8	1.074	0.218
(g)	12.75	0.375	7.003	0.469	4,100	65.6	89.7	83.5	0.931	0.58
(5)(c)	12.75	0.375	7.445	0.690	4,100	burst	95.5(d)	88.3	0.935	0.36
(g)	12.75	0.375	7.445	0.690	4,100	65.6	56.2(d)	53.5	0.952	0.889
(5)	18.00	0.375	3.00	0.188	2,330	burst	77.8	85.5	1.099	(b)
(5)	18.00	0.375	4.00	0.188	2,330	burst	99.0	100.5	1.015	0.116
(5)	18.00	0.375	4.00	0.250	2,330	burst	89.6	92.6	1.033	0.24
(5)	18.00	0.375	4.00	0.375	2,330	burst	73.3	73.0	0.996	0.584
(5)(c)	18.00	0.375	6.00	0.250	2,330	burst	113.2	120.4	1.064	0.127(c)
(5)(c)	18.00	0.375	6.00	0.375	2,330	burst	87.0	95.5	1.098	0.325(c)
(5)	8.625	0.322	8.625	0.322	4,600	burst	132.3	147.3	1.113	0.042(e)
(5)	8.625	0.322	4.50	0.237	4,600	burst	111.7	122.0	1.092	0.118
(5)	8.625	0.500	8.625	0.500	7,220	58.7	111.5	121.4	1.089	0.041(e)
(5)(c)	12.75	0.687	6.625	0.432	6,760	59.4	105.7	113.5	1.074	0.082(c)
(5)	24.00	0.312	4.50	0.237	1,970	79.9	129.8	141.2	1.088	0.419
(g)	24.00	0.312	4.50	0.237	1,970	79.9	109.5	108.2	0.988	0.520
(5)	24.00	0.312	12.75	0.250	1,580	84.3	194.4	241.3	1.241	0.269
(g)	24.00	0.312	12.75	0.250	1,580	84.3	161.8	182.7	1.129	0.450
(5)	24.00	0.312	24.0	0.312	1,620	84.3	247.8	285.1	1.151	0.208(e)(c)
(5)	5.983	0.193	3.59	0.116	3,250	62.4	132.6	130.3	0.983	(b)
(5)	24.00	0.104	12.75	0.102	225	49.0	123.5	205.8	1.666	0.60
(5)	12.50	0.281	10.5	0.250	2,200	60.9	150.4	151.6	1.008	0.028(c)
(5)	6.50	0.176	4.50	0.144	2,920	61.1	136.2	150.9	1.108	0.075(c)
(5)(f)	4.50	0.237	1.32	0.133	6,350	60.3	78.1	79.7	1.020	(b)
(5)	4.50	0.237	2.38	0.154	6,175	60.4	95.6	105.7	1.106	(b)
(5)	4.50	0.237	3.50	0.216	6,100	60.3	92.8	102.8	1.108	0.148
(5)	4.50	0.237	4.50	0.237	5,300	69.0	85.9	103.2	1.201	0.464
	61.5	0.75	12.75	0.688	350	17.1	23.3	26.4	1.133	0.674
	61.5	0.75	3.50	0.216	350	17.1	21.4	19.9	0.930	0.455

Table 1: Comparison of Design Methods for Integrally Reinforced Radial Nozzle to Cylinder Connections

Notes:

(a) VIII-1 reinforcement calculations for burst test cases performed using $S_v = S_n = 60$ ksi. For all other cases $S_v = S_n = S_u$ was used.

(b) Exempt from reinforcement calculations per UG-36(c)(3)(a).

(c) Actually failed 90 degrees from the assumed maximum stress location.

(d) FEA model indicated that the maximum membrane stress was located approximately 45 degrees from the assumed maximum stress location.

(e) VIII-1 rules would require a U-2(g) analysis instead of reinforcement calculations as $R_n/R > 0.7$.

(f) Failure occurred in the vessel in a location remote from the connection.

(g) Includes a nozzle internal projection of 1.0”.

Ref. No.	D_O in	T in	d_O in	t in	W in	t_e in	P psi	S ksi	P_L FEA ksi	P_L proposed ksi	Ratio	Aa/Ar VIII-1 (a)
(5)(b)	12.75	0.375	6.625	0.28	2.15	0.125	4,440	73.2	127.7(d)	124.1	0.972	0.31(f)
(5)	8.625	0.500	8.625	0.500	4.313	0.500	8,750	76.1	68.3	80.2	1.174	0.68(c)(f)
(5)	36.000	0.375	12.75	0.500	18.00	0.375	1,810	85.8	98.4	110.6	1.124	1.10(f)
(5)	36.000	0.675	12.75	0.500	18.00	0.675	3,115	85.8	86.9	99.4	1.144	0.72(f)
(6)	169.24	0.620	60.00	0.470	17.24	0.620	28	12.9(e)	11.0	11.5	1.046	7.40
(6)	169.24	0.620	60.00	0.470	17.24	0.620	57	25.2(e)	22.5	23.4	1.040	3.21
(6)	169.24	0.620	60.00	0.470	17.24	0.620	85	37.1(e)	33.5	34.9	1.042	1.82
(6)	169.24	0.620	60.00	0.470	17.24	0.620	114	48.4(g)	44.9	46.8	1.042	1.09
(h)	169.24	0.620	60.00	0.470	17.24	0.620	114		41.5	43.1	1.034	1.14
(6)	79.125	0.563	30.75	0.563	8.63	0.563	135	18.2(g)	18.6	18.0	0.968	2.53
(6)	79.125	0.563	30.75	0.563	8.63	0.563	273	42.7(g)	39.3	36.3	0.924	0.75
(h)	79.125	0.563	30.75	0.563	8.63	0.563	273		33.6	29.9	0.890	0.85
(6)	158.811	1.406	95.354	2.677	24.76	2.087	457	43.9(g)	39.0	33.7	0.864	0.71
(h)	158.811	1.406	95.354	2.677	24.76	2.087	457		33.5	30.1	0.899	0.78
	61.50	0.75	12.75	0.688	2.50	0.375	350		20.3	20.6	1.015	0.95
	61.50	0.75	12.75	0.688	5.00	0.25	350		21.4	20.6	0.963	1.03
	61.50	0.75	12.75	0.688	2.00	0.75	350		17.8(i)	16.1	0.904	1.25

Table 2: Comparison of Design Methods for Pad Reinforced Nozzle to Cylinder Connections

Notes:

(a) VIII-1 calculation performed using $S_v = S_n = S_p = 20$ ksi for SA-516 70.

(b) Burst test model failed in longitudinal plane.

(c) VIII-1 rules would require a U-2(g) analysis instead of reinforcement calculations as $R_n/R > 0.7$.

(d) Some uncertainty exists in the interpretation of the FEA model in these cases as higher localized stresses were reported at the pad to vessel fillet welds. The values listed are the FEA stresses slightly removed from the toe of the weld.

(e) From average strain gauge measurement reported by ref. 6.

(f) VIII-1 reinforcement calculations performed using $S_v = S_n = S_p = S$.

(g) Calculated from strain gauge measurements reported by ref. (6).

(h) Includes a nozzle internal projection of 2”.

(i) FEA model indicated that the maximum membrane stress was located approximately 45 degrees from the assumed maximum stress location.

Appendix A - September 1, 2000

Subsequent to publication, further verification of the method outlined in the paper has been performed. The purpose of this Appendix is to present a comparison between linear elastic FEA and the proposed method over a wider range of geometries. Calculations (in the form of area required divided by area available) using the ASME Code, A99 Addenda of Division 1 and Division 2 are also presented for comparison. Note that "duplicate" D/t ratios in the graphs represent different shell and nozzle diameter/thickness combinations.

As a result of this investigation it seemed desirable to add two additional geometric limitations to the method presented in the original paper as follows:

A2: $LH \le 8*T$

A3: h = lesser of the inside nozzle projection or $8*(T + te)$

These limits provide better agreement between the proposed method and FEA for the case of a thick nozzle attached to a very thin shell.

The following explanation of the reasoning behind the variable limits of reinforcement in the calculation of A1 may also prove helpful. The equation to use when calculating Lr changes depending on whether or not a reinforcement pad is present and also on the width and thickness of the pad itself. This is based on the FEA observation that if the pad is large enough it behaves locally like a thicker shell. It should be pointed out that the FEA excludes any stress analysis in the nozzle attachment welds. In the author's opinion this means that in order to take advantage of the larger A1 limit ($LR = 8*(T+te)$), a full penetration pad to nozzle weld should be used.

Graphical results of this additional verification follow for 6 inch, 12 inch and 24 inch schedule 80 nozzles.

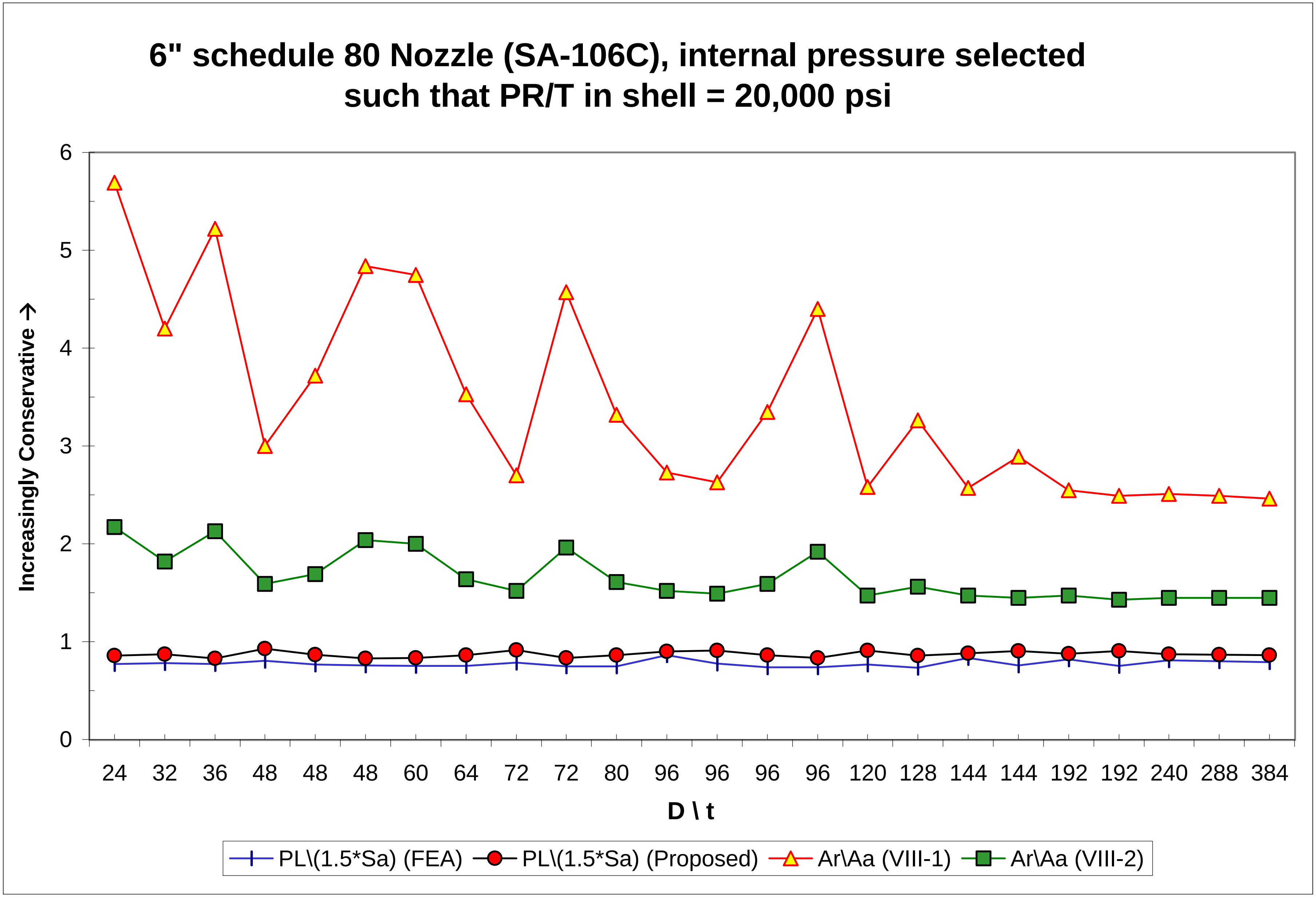
6" schedule 80 Nozzle (SA-106C), internal pressure selected such that PR/T in shell = 20,000 psi
Increasingly Conservative →
0
1
2
3
4
5
6
24 32 36 48 48 48 60 64 72 72 80 96 96 96 96 120 128 144 144 192 192 240 288 384
D \ t
PL\(1.5*Sa) (FEA)
PL\(1.5*Sa) (Proposed)
Ar\Aa (VIII-1)
Ar\Aa (VIII-2)

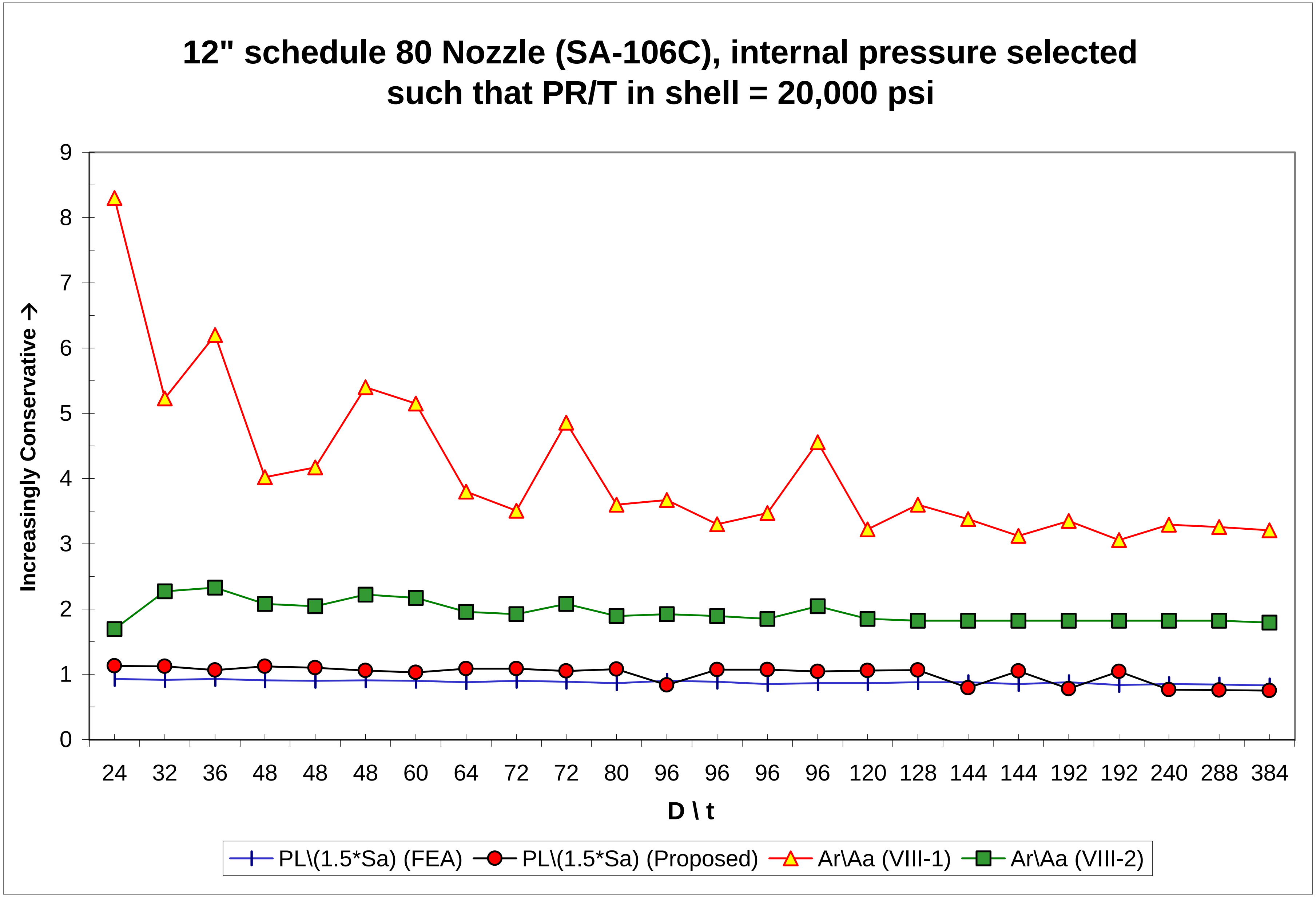

12" schedule 80 Nozzle (SA-106C), internal pressure selected such that PR/T in shell = 20,000 psi
Increasingly Conservative →
0
1
2
3
4
5
6
7
8
9
24 32 36 48 48 48 60 64 72 72 80 96 96 96 96 120 128 144 144 192 192 240 288 384
D \ t
PL\(1.5*Sa) (FEA)
PL\(1.5*Sa) (Proposed)
Ar\Aa (VIII-1)
Ar\Aa (VIII-2)

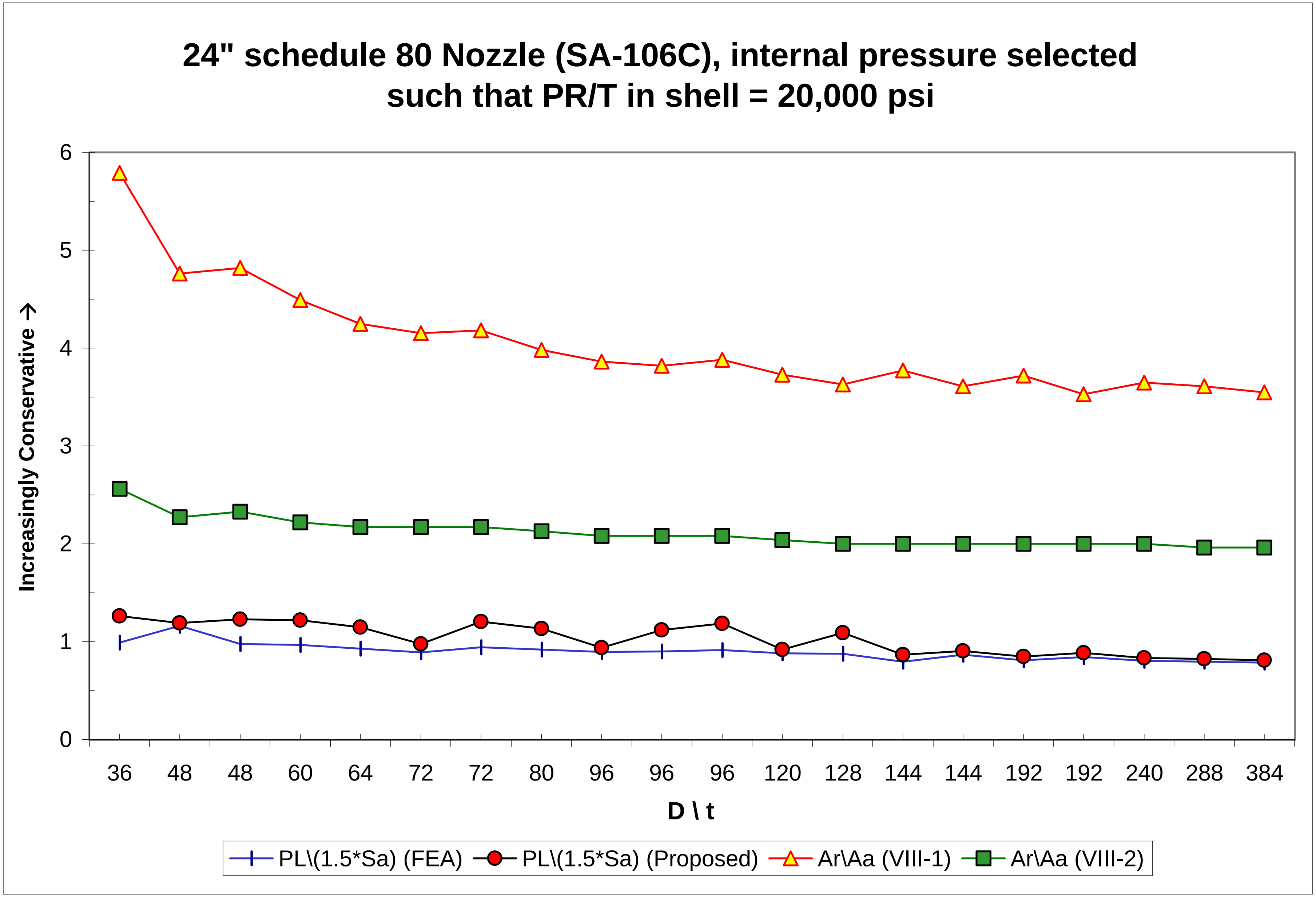
24" schedule 80 Nozzle (SA-106C), internal pressure selected
such that PR/T in shell = 20,000 psi
Increasingly Conservative →
0
1
2
3
4
5
6
36
48
48
60
64
72
72
80
96
96
96
120
128
144
144
192
192
240
288
384
D \ t
PL\(1.5*Sa) (FEA)
PL\(1.5*Sa) (Proposed)
Ar\Aa (VIII-1)
Ar\Aa (VIII-2)